Use of a fictitious Marangoni number for natural convection simulation

Francisco J. Arias* and Geoffrey T. Parks
Department of Engineering, University of Cambridge
Trumpington Street, Cambridge, CB2 1PZ, United Kingdom

In this paper, a method based on the use of a fictitious Marangoni number is proposed for the simulation of natural thermocapillary convection as an alternative to the traditional effective diffusivity approach. The fundamental difference between these two methods is that the new method adopts convective mass flows in simulating natural convection. Heat transfer in the natural convection simulation is calculated through the mass transport. Therefore, empirical Nusselt numbers correlations required in the effective diffusivity method are eliminated. This represents a clear advantage in the context of design studies where flexibility in varying the geometry unconstrained by the availability of appropriate correlations is highly desirable. The new method is demonstrated using a simple geometrical model. An analytical expression of the fictitious Marangoni number associated with convection between vertical plates is derived and a computational fluid dynamics (CFD) simulation is performed to study the efficacy of the proposed method. The results show that the new method can approximate real natural convection quite accurately and can be used to simulate the convective flow in complex, obstructed or finned structures where the specific Nusselt correlation is not known.

Keywords. *Natural convection, Effective thermal conductivity, Marangoni convection, Computational Fluid Dynamics (CFD)*

I. INTRODUCTION

Natural convection in enclosed cavities is of great importance in many engineering and scientific applications such as energy transfer, boilers, nuclear reactor systems, energy storage devices, etc. In the design of such systems numerical simulation using computational fluid dynamics (CFD) and experimental testing of prototypes are extensively used. However, these methods are not well suited to activities such as parametric analysis due to their time-consuming nature and high cost [1].

Natural convection analysis often involves complex simulations. Such simulations entail a set of relaxation factors to converge and no easy way to find the relaxation factors except through continuous trials demanding significant computational resources. This frequently dissuades thermal analysts and designers from attempting 3D simulations. In order to overcome this problem, the traditional approach is to use an effective diffusivity term (effective thermal conductivity) to convert effects of convection into pure conduction [2, 3]. The fluid within an enclosure behaves like a fluid the thermal conductivity κ of which is modified by an effective thermal conductivity κ_{eff} as $\kappa_{\text{eff}} = \kappa \cdot \mathbf{Nu}$, with the Nusselt number $\mathbf{Nu}$ being determined by an appropriate correlation. This provides a challenge to engineers when they are designing a complex or novel system. The engineers must have knowledge of the appropriate Nusselt number correlation relationship for the specific geometry, such as finned structures; however, these correlations are often not available. This then motivates us to find an alternative approach that does not require knowledge of Nusselt number correlations.

In this paper, an alternative approach is proposed for natural convection simulations in which the *momentum equation* is modified and then the mass flow represented by using a fictitious Marangoni term in the stress tensor inducing thermocapillary currents. The heat transfer is then the result of this mass flow. In the next section the theoretical background behind the proposed approach will be presented. Although prior knowledge of Marangoni convection is not essential to understand the material presented in the next section, the interested reader is referred to the text by Kuhlmann and Rath [4] for further information about fundamental Marangoni theory and to recent research outputs [5–14] and the book by Lappa [15] to obtain an overview of thermal convection and the state of the art.

II. THEORETICAL BACKGROUND

A. The fictitious Marangoni approach (FMA)

Let us start by considering the Navier-Stokes equation, which has, in presence of a gravitational field, the following tensorial form

$$\left(\frac{\partial v_i}{\partial t} + v_k \frac{\partial v_i}{\partial x_k}\right) = -\frac{1}{\rho}\frac{\partial p}{\partial x_i} + \frac{\partial}{\partial x_k}\{\sigma'_{ik}\} + g_i \quad (1)$$

*Corresponding author: Tel.: +32 14 33 21 94; Electronic address: fja30@cam.ac.uk

where v is the velocity, p is the static pressure, σ'_{ik} is the viscous stress tension (described below), and g_i is the gravitational body force per unit volume.

The viscous stress tensor is given by

$$\sigma'_{ik} = \eta\left(\frac{\partial v_i}{\partial x_k} + \frac{\partial v_k}{\partial x_i} - \frac{2}{3}\delta_{ik}\frac{\partial v_l}{\partial x_l}\right) \tag{2}$$

where η is the dynamic viscosity and δ_{ik} is the Kronecker delta.

Now let us derive the equation describing the natural convection. For the sake of simplicity, we will assume the fluid is incompressible. This assumption implies that the variation of density due to variation in pressure may be neglected. We can express the variations in temperature, density and pressure as functions of small variations dT, $d\rho$ and dp, respectively. This is the well-known Boussinesq approximation (for buoyancy). Introducing this into the Navier-Stokes equation (Eq. (1)), results in the following expression [16]:

$$\left(\frac{\partial v_i}{\partial t} + v_k\frac{\partial v_i}{\partial x_k}\right) = -\frac{1}{\rho}\frac{\partial dp}{\partial x_i} + \frac{\partial}{\partial x_k}\left\{\sigma'_{ik}\right\} - \beta dT g_i \tag{3}$$

where, with our assumption that the fluid is incompressible, i.e. $div \cdot u = 0$, the stress tensor is simplified as

$$\sigma'_{ik} = \eta\left(\frac{\partial v_i}{\partial x_k} + \frac{\partial v_k}{\partial x_i}\right) \tag{4}$$

Let us now consider the situation of a boundary condition that must be satisfied at the boundary between the fluid and the walls, when surface-tension forces are taken into account. If we assume that the surface-tension coefficient γ is not constant over the surface (in our case because of temperature variation), then a force tangential to the surface is developed $\frac{\partial\gamma}{\partial x_i}$, and the stress tensor then becomes

$$\sigma'_{ik} = \eta\left(\frac{\partial v_i}{\partial x_k} + \frac{\partial v_k}{\partial x_i}\right) + \frac{\partial\gamma}{\partial x_i} \tag{5}$$

Now, our objective in this paper is to define a fictitious surface-tension gradient, $\partial\gamma/\partial x_i$, which emulates the buoyancy potential, $\beta dT g_i$. Although there are several ways in which to do this, perhaps the following analogy is easiest in applying this approach to cases involving plates and finned structures.

In laminar, fully developed, two-dimensional (2D) flow between parallel plates (see Fig. 1), the pressure drop is given by [16]

$$\left.\frac{dp}{dx_i}\right|_{\text{loss}} = -2\frac{\sigma'_{ik}}{s} \tag{6}$$

where s is the distance between the plates and the stress tensor is given by

$$\sigma'_{ik} = \eta\left(\frac{\partial v_i}{\partial x_k}\right)_{x_k=0} \tag{7}$$

or, considering the velocity profile between the parallel plates [17],

$$\left.\frac{dp}{dx_i}\right|_{\text{loss}} = -12\frac{\eta w}{\rho s^3} \tag{8}$$

where w is the mass flow rate per unit of width.

For natural convection flow, this flow resistance is balanced by the buoyant potential [17] given by

$$\left.\frac{dp}{dx_i}\right|_{\text{buoy}} = -\rho\beta dT g_i \tag{9}$$

Equating the dp/dx_i terms in Eq. (8) and Eq. (9) we obtain the well-known solution given by Bar-Cohen and Rohsenow [18] for the mass flow rate per unit width in the channel:

$$w = \frac{\rho^2 g_i \beta s^3 dT}{12\eta} \tag{10}$$

As mentioned, we want to find an appropriate fictitious surface-tension gradient $\partial\gamma/\partial x_i$. In this case, using Eqs. (5) and (7), we can write the stress tensor as

$$\sigma'_{ik} = \eta\left(\frac{\partial v_i}{\partial x_k}\right)_{x_k=0} = \frac{\partial\gamma*}{\partial x_i} \tag{11}$$

where $\partial\gamma*/\partial x_i$ is the fictitious surface-tension gradient associated with the wall.

Taking into account Eqs. (6), (9) and (11) we find that the fictitious surface-tension gradient must be given by

$$\frac{\partial\gamma*}{\partial x_i} = \frac{\rho\beta g_i s dT}{2} \tag{12}$$

Given that

$$\frac{\partial\gamma*}{\partial x_i} = \frac{\partial\gamma*}{\partial T_s}\partial_s T \tag{13}$$

where $\partial_s T = \partial T_s/\partial x_i$ and the subscript s means that the temperature is evaluated at the wall, Eqs. (12) and (13) can be combined to give

$$\frac{\partial\gamma*}{\partial T_s} = \frac{\rho\beta g_i s}{2}\left[\frac{dT}{\partial_s T}\right] \tag{14}$$

Using the definitions of the Rayleigh number $\mathbf{Ra}_s$ and the Marangoni number $\mathbf{Ma}$:

$$\mathbf{Ra}_s = \frac{\rho\beta g_i s^3}{\eta\alpha} dT \tag{15}$$

$$\mathbf{Ma} = -\frac{\partial\gamma*}{\partial T_s}\frac{h dT}{\eta\alpha} \tag{16}$$

where α is the thermal diffusivity and h is a characteristic length, here the length of the channel, Eq. (14) can then be rewritten as

$$\mathbf{Ma} = \frac{C_1}{2}\left[\frac{\partial_f T}{\partial_s T}\right]\mathbf{Ra}_s \tag{17}$$

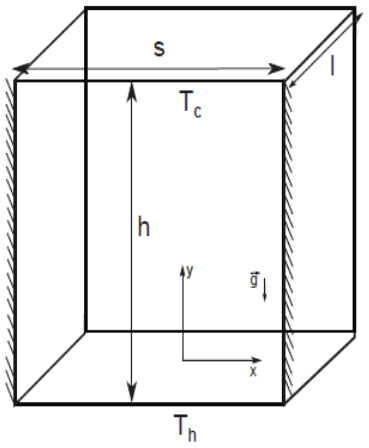

FIG. 1: Simulated cavity model with a bottom wall temperature of T_h, a top wall temperature of T_c and adiabatic side walls.

where $\partial_f T = dT/h$ is the linear average fluid temperature gradient and C_1 is a geometry-dependent constant.

Eq. (17) presents a relationship between the fictitious Marangoni number and the Rayleigh number. The difference between these two dimensionless numbers relates to mechanism by which natural convection is initiated. The Marangoni number is associated with natural convection caused by a surface temperature gradient $\nabla_s T$ via mass transfer while the Rayleigh number is associated with natural convection caused by buoyancy-driven flow. This equation provides an important result. The Nusselt number correlation, which is required in the traditional effective diffusive approach, is no longer required. It can be replaced by a ratio $\nabla_f T/\nabla_s T$ that is determined by the specific geometry.

For the sake of generality, the relationship between the fictitious Marangoni number and the Rayleigh number can be expressed through a simple polytropic equation:

$$\mathbf{Ma} = C_1 \mathbf{Ra}^n \tag{18}$$

where C_1 and n are constants. Based on Eq. (17), n would be expected to be close to 1. The value of C_1 depends on the specified geometry.

If the surface temperature gradient $\nabla_s T$ is assumed to be proportional to the thermal gradient of the fluid then:

$$\partial_s T \approx C_1 \frac{dT}{s} \tag{19}$$

In the Appendix a simple application for a finned geometry is presented, for which the existence of a simple linear relationship between the surface temperature gradient $\nabla_s T$ and the thermal gradient can be demonstrated. Combining Eq. (19) with Eq. (14) then yields

$$\frac{\partial \gamma*}{\partial T_s} \approx C_1 \frac{\rho \beta g_i s^2}{2} \tag{20}$$

All parameters in this equation are known once the geometry is specified. This then enables natural convection to be simulated without knowledge of the appropriate Nusselt number correlation.

B. The effective diffusivity approach (EDA)

In the previous section we propose a new approach for natural convection simulation based on the introduction of a "fictitious" Marangoni term in the stress tensor in the *momentum equations*. In this proposed approach heat transfer will be obtained as a result of the induced mass flow.

In contrast, the problem of computational natural convection simulation is often these days tackled from a totally different point of view using more traditional approaches. Instead of modifying the *momentum equations* (and then considering mass transport) it is the *energy equation* that is modified. There are several approaches to representing the effects of convection by modifying the energy equation: for example, by introducing empirical velocities into the convection terms in the energy equation [19]. However, undoubtedly the most commonly used approach of this kind is the so-called effective diffusive approach, so it is worth providing a brief outline of that model here.

Let us consider the energy equation, and for the sake of illustration, let us assume, as before, laminar flow in the liquid where no external sources are present. The energy equation is given by

$$c_p \frac{\partial T}{\partial t} + v_i \frac{\partial T}{\partial x_i} = \frac{1}{\rho} \frac{\partial}{\partial x_i} \left(\kappa \frac{\partial T}{\partial x_i} \right) \tag{21}$$

where c_p is the specific heat capacity of the fluid. The convective term in the above equation ($v_i \frac{\partial T}{\partial x_i}$) makes it difficult to solve computationally, so it is modeled as an effective diffusive term as [20]

$$v_i \frac{\partial T}{\partial x_i} = -\frac{1}{\rho} \frac{\partial}{\partial x_i} \left(D \frac{\partial T}{\partial x_i} \right) \tag{22}$$

where

$$D = \kappa C \mathbf{Ra}^a \tag{23}$$

or

$$D = \kappa \mathbf{Nu} \tag{24}$$

In this way, it is possible to eliminate the non-linear convective term in the energy equation (Eq. (21)), representing the energy equation for a simple purely conductive system [21]

$$c_p \frac{\partial T}{\partial t} = \frac{1}{\rho} \frac{\partial}{\partial x_i} \left(\kappa_{\text{eff}} \frac{\partial T}{\partial x_i} \right) \tag{25}$$

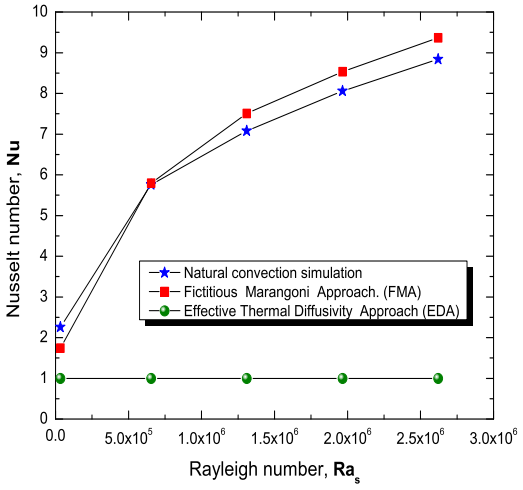

FIG. 2: Comparison of the Nusselt number predictions.

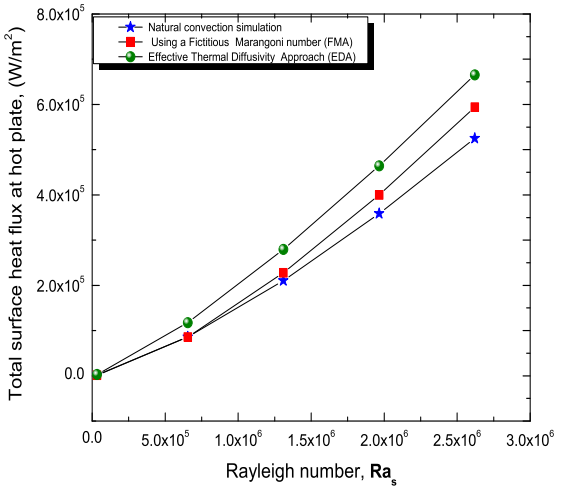

FIG. 3: Comparison of the total surface heat flux predictions.

C. FMA versus EDA

In the previous section, two different alternative approaches for natural convection simulation were described. The first, proposed in this paper, is through the modification of the *momentum equations* by the introduction of a fictitious Marangoni stress (Eq. (20)), an approach that we have called the fictitious Marangoni approach or FMA. The second is the traditional effective diffusivity approach or EDA, in which the *energy equation* is modified by replacing the convective term by an effective diffusive term (Eq. (22)).

As will be apparent to the reader, the FMA approach offers a powerful tool for systems where, because the Nusselt number is not known, it is not possible to define an effective thermal diffusivity (thermal conductivity), i.e. to apply the EDA directly. Such a situation frequently arises in the simulation of complex designs with dramatic variations in geometry (e.g. in the microelectronics field) where there is no available Nusselt number correlation for the specific system available in handbooks or the literature, thus forcing thermal engineers adopting the EDA to use the Nusselt number correlation for the most similar geometry available. If this is not a good approximation, poor results are inevitable.

Thus the FMA can be used either as a method for the simulation of natural convection, or at least as a tool for pre-screening and obtaining an estimate of the Nusselt number, which can then be used in applying the EDA. In the next section, we will examine a numerical comparison between these models.

III. RESULTS AND DISCUSSION

In order to demonstrate the efficacy of the proposed FMA method, a computational fluid dynamics (CFD) analysis using **FLUENT-6.3®** was performed on a simple cavity model (see Fig. 1) consisting of a square box with a hot bottom wall, a cold top wall and adiabatic side walls. Gravity acted downwards. The values of physical properties and operating conditions (e.g. the gravitational acceleration) were adjusted according to the desired Rayleigh number [22]. In this study, the values were chosen as: $\rho = 1000$ kg/m^3, $c_p = 11.030$ kJ/kgK, $\kappa = 15.309$ W/mK, $\eta = 10^{-3}$ kg/ms, $\beta = 10^{-5}$, $g_i = 6.96 \times 10^{-5}$ m/s^2, $h = l = s = 1$ m.

The case was set with a pressure-based, segregated, steady solver with Green-Gauss cell-based gradient treatment. The Semi-Implicit Method for Pressure Linked Equations (SIMPLE) algorithm was selected for the pressure-velocity coupling with relaxation factors of 0.3 for pressure, 0.7 for momentum and 1 for energy as the defaults. The pressure was discretized with a standard Rhie-Chow discretisation scheme [23] and and Quadratic Upstream Interpolation for Convective Kinematics (QUICK) was chosen as the advection scheme for momentum and energy discretization. The convergence criteria were set for absolute residuals below 1×10^{-7} for all the variables in all cases and the overall imbalance in the domain was less than 1% for all variables, then convergence of the solution was checked at each time step by using the scaled residuals. The mesh resolution independence was checked running an initial mesh and ensuring that the convergency criteria of RMS of 10^{-7}, and an imbalance in the domain was less than 1%, then, a second simulation was performed using a second mesh with finer cells throughout the domain, then the sim-

ulation was run until the convergency criteria and imbalance in the domain were satisfied. The criteria for selection of the mesh was that the temperature values for two consecutive stimulations were less than a 1%, then the mesh at the previous step was considered accurate enough to capture the result. Finally, time step independence was achieved using time-steps of 0.5 s. The temperature difference between the top and bottom walls was set based on Rayleigh numbers of $\mathbf{Ra} = 3.28 \times 10^4$, 6.55×10^5, 1.31×10^6, 1.97×10^6 and 2.62×10^6. Simulations were performed at each Rayleigh number for three cases: **1)** a real natural convection simulation; **2)** using the proposed FMA; and **3)** using the traditional EDA. For the FMA cases, the gravitational acceleration was set to zero and Eq. (20) was used for the effective surface tension gradient with the best fit using $C_1 = 0.06$ and $\partial\gamma*/\partial T_s = 1.2 \times 10^{-8}$ N/mK. For the EDA cases, the effective thermal diffusivity was calculated using

$$\kappa_{\text{eff}} = \kappa \mathbf{Nu} \tag{26}$$

where the Nusselt number was calculated from [21]

$$\mathbf{Nu} = 0.27\mathbf{Ra}_s^{\frac{1}{4}} \tag{27}$$

Figs. 2 and 3 show comparisons between the Nusselt numbers and the total heat fluxes at various channel Rayleigh numbers for the three cases. It is found that the proposed FMA-based method can track the real natural convection simulation far better than the traditional EDA-based method.

Figs. 4–6 further demonstrate the advantage of the proposed FMA-based method via comparison of the temperature distributions obtained for the convection simulations. It is obvious that the temperature distribution obtained using the FMA agrees much better with the real natural convection CFD simulation than that given by the EDA-based method.

The advantage of the proposed FMA method is due its use of mass transfer. The FMA method emulates the convective flow via mass transport which is associated with the momentum balance. This method can easily take into consideration the effect on mass transfer of the real geometry of the system. It provides a powerful tool for the simulation of 2D natural convection in complex geometries such as finned structures, obstruction-type structures and generally dramatically varying geometries for which the Nusselt number correlation is unknown. In contrast, the EDA method relies on knowledge of the Nusselt number correlation which can vary significantly with subtle changes in geometry. In particular, when the real geometry has unusual shapes or variations from standard shapes, it is hard to find an accurate Nusselt number correlation in the literature for the specific geometry.

As mentioned before, there is a certain trick behind the apparently good results given through the use of the EDA depicted in Fig. 3, a trick that is also a weakness. The good results are basically due to the introduction of the Nusselt number correlation, but in a way that is

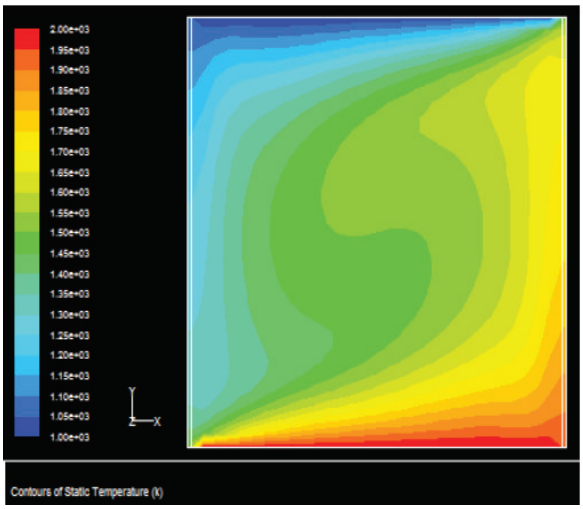

FIG. 4: Temperature distribution calculated using the proposed FMA-based method.

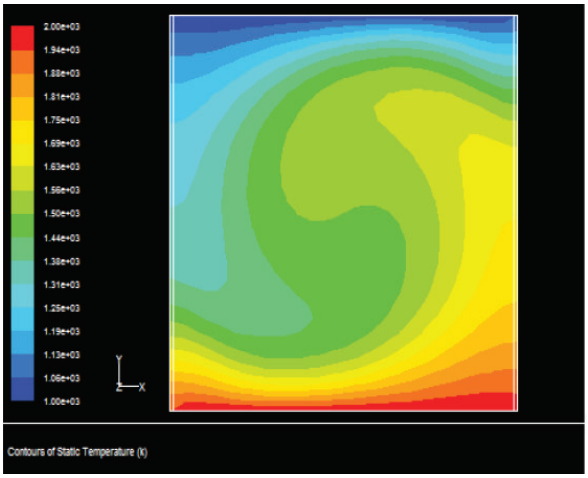

FIG. 5: Temperature distribution of the real natural convection CFD simulation.

precisely what we are trying to calculate. So, if we introduce a geometrical variation and re-launch the same calculations, the weakness of the EDA is exposed and the difference between it and the proposed FMA is made manifestly clear.

To illustrate, let us consider the case of the cavity model shown in Fig. 1 where now the flow is obstructed by a sphere of radius 0.5 m located at the center of the cavity. The calculated results for the total surface heat flux in this new scenario are shown in Fig. 7. It is clear that the effect on the natural convection of the modification to the system geometry can be easily and well

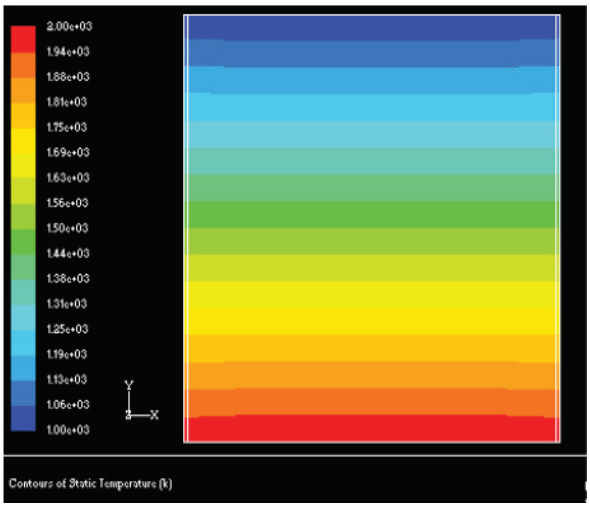

FIG. 6: Temperature distribution calculated using the traditional EDA-based method.

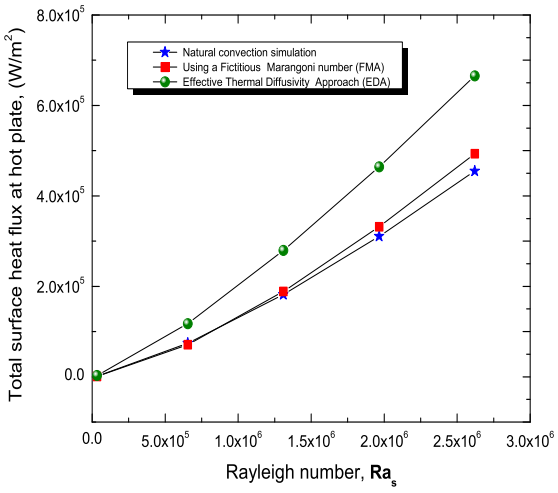

FIG. 7: Comparison of the total surface heat flux predictions for the case of a cavity with a sphere of radius 0.5 m at its center.

captured by the FMA method. However, the results obtained from the EDA method are unchanged (and therefore now very inaccurate) if the same Nusselt number correlation as before is used (as has been done here).

If a more appropriate Nusselt number correlation is known then, of course, it can be used with the EDA method instead and improved results will follow, but such an adjustment is only possible if the new correlation is known. Restricting the thermal engineer/designer to the consideration of geometries for which correlations are already known will severely limit the range of system designs can that be analysed and may well exclude the optimal geometry for the application in question.

IV. CONCLUSIONS

A fictitious Marangoni number method has been proposed and demonstrated for 2D natural convection simulation. It was shown that the proposed method is much superior to the traditional effective thermal diffusivity approach often used in 1D or 2D modeling of natural convection. The key conclusions are:

- The proposed fictitious Marangoni number method can realistically simulate convective flow via mass transport and does not rely on prior knowledge of any empirical Nusselt number correlations. It can model the real natural convection flow field accurately.

- The proposed fictitious Marangoni number method can easily incorporate the effects of the system geometry (and changes to that geometry) on natural convection simulation. It eliminates the disadvantage of the traditional effective thermal diffusivity approach which requires knowledge of the Nusselt number correlations associated with different geometries. The new method is especially suitable for application to complex geometries.

- A further advantage of the proposed fictitious Marangoni number method is the possibility that it can be applied not just to steady-state convection simulation but also to transient cases where the surface temperature profile follows the bulk temperature profile of the fluid and thus the relationship between these used in the definition of the fictitious Marangoni number is maintained during the transient. Such a relationship may hold (to a good approximation) in many transient cases where no abrupt changes take place. Additional research is required to investigate the applications and limitations of this novel approach in simulating natural convection transients.

V. APPENDIX

A. Finned geometries

In the main body of the paper, for the sake of illustration, it was assumed that there was a simple linear relationship between the surface temperature gradient $\partial_s T$ and the thermal gradient in the fluid $\partial_f T$ (see Eq. (19)). Although the specific relationship between $\partial_s T$ and $\partial_f T$ will depend on the specified geometry, we demonstrate here in a more rigorous way that for finned geometries a linear approximation is good enough for preliminary calculations.

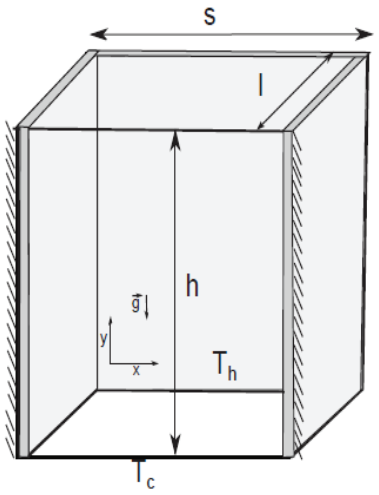

FIG. 8: Detail of the straight rectangular fin studied.

Let us consider, as an example, the straight rectangular fin depicted in Fig. 8. Assuming that the Marangoni stress will act on all the available walls, then from momentum balance considerations

$$(2hl + sh)\sigma'_{ik} = -\rho\beta g_i \Delta T(hsl) \tag{28}$$

where $\Delta T = T_h - T_c$. The fictitious surface tension gradient then gives

$$\frac{\partial\gamma*}{\partial T_s} = \left[\frac{ls}{2l+s}\right]\frac{\rho\beta g_i dT}{\partial T_s} \tag{29}$$

The only unknown parameter in Eq. (29) is the surface temperature gradient ∂T_s which can be calculated from the following considerations. The temperature distribution profile along the length of a fin of finite length l with an insulated end can be expressed as [24]

$$T(z) - T_a = [T_0 - T_a]\frac{\cosh(m(l-z))}{\cosh(ml)} \tag{30}$$

where T_0 is the temperature at the base of the fin and T_a is the ambient temperature, and

$$m = \sqrt{\frac{h_f P}{\kappa A_c}} \tag{31}$$

where h_f is the heat transfer coefficient along the fin, P is the perimeter of the fin and A_c is its base-area. Although Eq. (30) is valid for a fin of finite length with an insulated end and in general the end of a fin is not insulated, this is a good approximation if the heat transfer from the end of the fin is negligible in comparison to the heat transfer from the surface of the fin, a common situation since the area of the end of a fin is frequently negligible in comparison to the total exposed surface area [24].

Differentiating Eq. (30), the surface temperature gradient along the fin is

$$\partial_s T = -[T_0 - T_a]m \cdot \frac{\sinh(m(l-z))}{\cosh(ml)} \tag{32}$$

The fin efficiency η_{fin} is defined as the ratio of the heat transferred to that transferred for an infinitely long fin of the same cross-section. For this kind of fin η_{fin} is given by [21]

$$\eta_{\text{fin}} = \tanh(ml) \tag{33}$$

Thus, in practice, a fin length that corresponds to $ml \approx 1$ will transfer 76.2% of the heat that can be transferred by an infinitely long fin, and offers a good compromise between heat transfer performance and fin size [21]. So, assuming $ml = 1$, Eq. (32) becomes

$$\partial_s T = -0.648\frac{\Delta T}{l}\sinh\left(1 - \frac{z}{l}\right) \tag{34}$$

where $\Delta T = T_0 - T_a$. The function $f(z) = \sinh(1 - \frac{z}{l})$ is integrable on $[0, l]$. This an average value $\overline{f(z)}$ for z in the interval $[0, l]$ may be defined by:

$$\overline{f(z)} = \frac{1}{l}\int_0^l \sinh\left(1 - \frac{z}{l}\right) dz = 0.543 \tag{35}$$

Incorporating this value into Eq. (34) yields

$$\overline{\partial_s T} \approx -0.352\frac{\Delta T}{l} \tag{36}$$

Inserting Eq. (36) into Eq. (29), we have for our fictitious surface gradient

$$\frac{\partial\gamma*}{\partial T_s} = 2.85 C_1\left[\frac{l^2 s}{2l+s}\right]\rho\beta g_i \tag{37}$$

where a constant C_1 has been introduced to take into account the error introduced by the use of an average value from Eq. (34).

NOMENCLATURE

A_c = fin base-area
C_1 = constant
c_p = specific heat capacity
D = diffusion coefficient
g_i = gravitational acceleration
h = channel or plate length
h_f = heat transfer coefficient
l = plate width or fin length
m = fin temperature profile parameter
Ma = Marangoni number
n = exponent
Nu = Nusselt number
P = fin perimeter
Ra = Rayleigh number
s = plate spacing

T = temperature
v = velocity
w = mass flow per unit width
z = length coordinate

Greek symbols
α = thermal diffusivity
β = thermal expansion coefficient
$\gamma*$ = fictitious surface tension
κ = thermal conductivity
ρ = density
σ = surface tension
η = dynamic viscosity
η_{fin} = fin efficiency

Subscripts
a = ambient value
c = cold
eff = effective value
f = fluid
h = hot
i, j, k = coordinate directions
s = surface

REFERENCES

[1] P.M. Teertstra, M.M. Yovanovich, J.R. Culham, **Modeling of natural convection in electronic enclosures**. J. Electronic Packaging, 128 (2) (2006), pp. 157–165

[2] V.A. Bui, T.N. Dinh, Modeling of heat transfer in heat-generating liquid pools by an effective diffusivity-convectivity approach, in: Proceedings of 2nd European Thermal-Sciences Conference, Rome, Italy (1996), pp. 1365–1372

[3] F.B. Cheung, S.W. Shiah, D.H. Cho, M.J. Tan, **Modelling of heat transfer in a horizontal heat-generating layer by an effective diffusivity approach**. ASME HTD, 192 (1992), pp. 55–62

[4] H.C. Kuhlmann, H-J. Rath, **Free Surface Flows**, Springer Verlag GmbH, Vienna, Austria (1998)

[5] M. Wegener, **A numerical parameter study on the impact of Marangoni convection on the mass transfer at buoyancy-driven single droplets**. Int. J. Heat Mass Transfer, 71 (2014), pp. 769–778

[6] Z. Pan, H. Wang, **Bénard–Marangoni instability on evaporating menisci in capillary channels**. Int. J. Heat Mass Transfer, 63 (2013), pp. 239–248

[7] K. Li, Z.M. Tang, W.R. Hu, **Coupled thermocapillary convection on Marangoni convection in liquid layers with curved free surface**. Int. J. Heat Mass Transfer, 55 (9–10) (2012), pp. 2726–2729

[8] Z. Alloui, P. Vasseur, **Onset of Marangoni convection and multiple solutions in a power-law fluid layer under a zero gravity environment**. Int. J. Heat Mass Transfer, 58 (1–2) (2013), pp. 43–52

[9] K.M. Armijo, V.P. Carey, **An analytical and experimental study of heat pipe performance with a working fluid exhibiting strong concentration Marangoni effects**. Int. J. Heat Mass Transfer, 64 (2013), pp. 70–78

[10] E.A. Chinnov, **Wave – Thermocapillary effects in heated liquid films at high Reynolds numbers**. Int. J. Heat Mass Transfer, 71 (2014), pp. 106–116

[11] E. Lim, Y.M. Hung, **Thermocapillary flow in evaporating thin liquid films with long-wave evolution model**. Int. J. Heat Mass Transfer, 73 (2014), pp. 849–858

[12] S. Maity, **Thermocapillary flow of thin liquid film over a porous stretching sheet in presence of suction/injection**. Int. J. Heat Mass Transfer, 70 (2014), pp. 819–826

[13] T.C. Lee, H.J. Keh, **Axisymmetric thermocapillary migration of a fluid sphere in a spherical cavity**. Int. J. Heat Mass Transfer, 62 (2013), pp. 772–781

[14] P. Zhu, L. Duan, Q, Kang, **Transition to chaos in thermocapillary convection**. Int. J. Heat Mass Transfer, 57 (2) (2013), pp. 457–464

[15] M. Lappa, **Thermal Convection: Patterns, Evolution and Stability**, John Wiley & Sons, Chichester, UK (2010)

[16] L.D. Landau, E.M. Lifshitz, **Fluid Mechanics**, 2nd edition, Pergamon Press, Oxford, UK (1987)

[17] W.M. Rohsenow, H. Choi, **Heat, Mass and Momentum Transfer**, Prentice Hall, New Jersey (1961)

[18] A. Bar-Cohen. W.M. Rohsenow. **Thermally optimum spacing of vertical, natural convection cooled, parallel plates**. ASME J. Heat Transfer, 106 (1) (1984), pp. 116–123

[19] C.T. Tran, T.N. Dinh, **Simulation of core melt pool formation in a reactor pressure vessel lower head using an effective convective model**. Nucl. Eng. Technol., 41 (7) (2009), pp. 929–944

[20] A.J. Parry, P.C. Eames, F.B. Agyenim, **Modeling of thermal energy storage shell-and-tube heat exchanger**. Heat Transfer Eng., 35 (1) (2014), pp. 1–14

[21] Y.A. Çengel, A.J. Ghajar, **Heat and Mass Transfer, Fundamentals & Applications**, 4th Edition, McGraw Hill, New York (2007)

[22] **FLUENT 6.3 Tutorial Guide**, Chapter 5: Modeling Radiation and Natural Convection, Fluent Inc., Lebanon, New Hampshire (2006)

[23] C.M. Rhie, W.L. Chow, **Numerical study of the turbulent flow past an airfoil with trailing edge separation**. AIAA J., 21 (11) (1983), pp. 1525–1532

[24] M. Thirumaleshwar, **Fundamentals of Heat and Mass Transfer**, Pearson Education India, New Delhi, India (2006)